PHYSICAL REVIEW B VOLUME 13, NUMBER 8 15 APRIL 1976

Dielectric function in $Cd_x Hg_{1-x} Te$ mixed crystals

A. Polian, R. Le Toullec, and M. Balkanski
Laboratoire de Physique des Solides, Laboratoire associé au C.N.R.S. Université Pierre et Marie Curie, 4, Place Jussieu, 75230 Paris Cedex 05, France
(Received 28 April 1975)

Reflectivity spectra of $Cd_xHg_{1-x}Te$ mixed crystals are measured at 8 K in the far-infared spectral region: 40–125 μm with special emphasis on the semimetal-semiconductor transition ($x \simeq 0.15$). The dielectric function is analyzed as a sum of contributions: Electron interband transitions with the transitions $\Gamma_8 \rightarrow \Gamma_8$ for $x < 0.15$ and $\Gamma_8 \rightarrow \Gamma_6$ for $x > 0.15$, calculated within the assumption of nonparabolic bands; phonon contribution given by a two-mode behavior for ail x calculated with a phenomenological model taking into account long-range interactions and plasmon contribution. The experimental results can be accounted in the frame of the adiabatic approximation for all concentrations.

I. INTRODUCTION

In a recent investigation[1] on the dielectric function in HgTe, the reflectivity spectra in the region 80–250 cm^{-1} (40–125 μm) were analyzed in terms of electronic interband transitions, phonon contribution, and plasmon-phonon coupled modes. Plasmon-phonon dispersion was obtained as a function of the free-carrier concentration. The adiabatic approximation in this zero-gap semiconductor was questioned and it was found that the experimental results pointed to a breakdown of this approximation. Broerman[2] has given an extensive bibliography on dielectric-function anomalies in zero-gap compounds.

CdTe as a conventional semiconductor has its phonon and electron contributions to the dielectric function well separated and their coupling is not to be considered in the frequency range of interest.

It then becomes interesting to investigate the behavior of the dielectric function in the whole range of concentration of $Cd_xHg_{1-x}Te$ mixed crystals and check the applicability of the adiabatic approximation.

$Cd_xHg_{1-x}Te$ mixed crystals can be obtained in all compositions between the semimetal HgTe and the semiconductor CdTe. HgTe has a negative band gap $\Gamma_6 - \Gamma_8$ at low temperature: $E_G \simeq -0.3$ eV. This energy difference increases linearly with concentration x. It has a zero value for $x_0 \simeq 0.15$ for which the two bands Γ_6 and Γ_8 cross. For larger values of x the gap is positive ($E_{\Gamma_6} - E_{\Gamma_8}$) and increases with x.

For concentrations close to $x_0 = 0.15$ phonon excitation energies are of the order of the semimetal electronic interband transitions $\Gamma_8 \rightarrow \Gamma_8$ and of the semiconductor electronic interband transitions $\Gamma_8 \rightarrow \Gamma_6$. It is the spectral range of these transitions which is particularly explored in this paper.

Early infrared-reflectivity measurements at low[3] and high[4,5] temperatures have shown a two-mode behavior of the optical phonons. Raman-scattering measurements[6] at 1.7 K, infrared transmission, [7] and cyclotron resonance[8] in a Voigt configuration confirm the two-mode behavior, but in none of these investigations is a dispersion mode given for the optical constants. For HgTe such a model has been developed[1] by Grynberg, Le Toullec, and Balkanski who showed that, at low temperature, the electronic-interband-transitions contribution to the dielectric function is very strong and anomalous in the phonon frequency range.

In this paper we examine the dielectric function for all concentrations between $x = 0$ (HgTe) and $x = 1$ (CdTe) in terms of (i) Electronic interband transitions from the heavy-hole band to the conduction band: $\Gamma_8 \rightarrow \Gamma_8$ on the HgTe side, and $\Gamma_8 \rightarrow \Gamma_6$ on the CdTe side. This contribution is calculated in the framework of Kane's procedure to take into account the bands nonparabolicity. (ii) Phonon contribution in terms of two-mode behavior. A phenomenological model taking into account long-distance interactions is used to calculate the phonon spectrum. (iii) Plasmon contribution.

Hence the dielectric function can be taken as a sum of terms

$$\epsilon(\omega) = \epsilon_{\text{inter}} + \epsilon_{\text{phonon}} + \epsilon_{\text{intra}}.$$

Since the experimental curves are fully accounted for by the sum of these contributions, the adiabatic approximation is therefore applicable in the whole range of concentration. We then show that our model for the dielectric function is applicable as well in the semimetallic range $x < 0.15$ as in the semiconductor range $x > 0.15$.

II. THEORETICAL MODEL

The adiabatic approximation is applicable when the motion of ions and electrons is decoupled, that is, as a rule for wide-gap semiconductors, for instance CdTe. For small-gap or zero-gap semiconductors, the energy of interband electronic transitions is about the same order of magnitude as the energy of lattice vibrations and the applicabil-

ity of the adiabatic approximation has been questioned. Blinowski[9] has studied theoretically the electron-phonon interaction for small moments. His results show that the effect of this interaction upon the imaginary part of the dielectric function $\epsilon(\omega)$ will be a slight broadening of the optical-phonon maximum. This contribution will be negligible compared to other damping processes such as anharmonicity and the difference with the adiabatic case will not be accessible to experiment. Calculations of $Cd_xHg_{1-x}Te$ have therefore been done in this approximation.

The total polarization induced by the macroscopic field $\vec{E}$ is then a sum of the ionic and electronic contributions and the total dielectric function of the system in the low-frequency region will be

$$\epsilon(\omega) = \epsilon_{\text{inter}} + \Delta\epsilon_{\text{intra}} + \Delta\epsilon_{\text{ph}}, \tag{1}$$

ϵ_{inter} corresponds to interband electronic transitions, $\Delta\epsilon_{\text{intra}}$ corresponds to intraband transitions, $\Delta\epsilon_{\text{ph}}$ is the polar-optical-phonon contribution.

In the far infrared, photon energies are much smaller than that of the optical gaps E_0 of classical semiconductors. For CdTe, $\hbar\omega_{TO} = 0.017$ eV and $E_0 \simeq E_G = 1.6$ eV. The interband transitions contribution is therefore nearly constant at these energies. For semimetals and small-gap semiconductors, the optical gap may have an energy of the same order as that of optical phonons. The interband contribution will therefore be a function of energy in the far infrared. This interband contribution $\Delta\epsilon_{\text{inter}}(\omega)$ will be separated from the contribution from other high-energy interband processes which contribute a constant term to the dielectric function in the low-energy regime[10]:

$$\epsilon_{\text{inter}} = \Delta\epsilon_{\text{inter}}(\omega) + \epsilon_\infty. \tag{2}$$

In the $Cd_xHg_{1-x}Te$ series, all these contributions are functions of x. In our model, we will therefore write

$$\epsilon(x, \omega) = \epsilon_\infty(x) + \Delta\epsilon_{\text{inter}}(x, \omega) + \Delta\epsilon_{\text{intra}}(x, \omega) + \Delta\epsilon_{\text{ph}}(x, \omega). \tag{3}$$

A. Interband contribution $\Delta\epsilon_{\text{inter}}(x,\omega)$

An explicit expression for $\Delta\epsilon_{\text{inter}}(x, \omega)$ can be obtained in the random-phase approximation (RPA). The imaginary part of $\Delta\epsilon_{\text{inter}}$ can then be written in the form[2]

$$\Delta\epsilon''_{\text{inter}} = \lim_{q\to 0} -\frac{e^2}{\pi^2 q^2}\int d^3k \left|\langle \vec{k}+\vec{q},\ c \left| e^{-i\vec{q}\cdot\vec{r}} \right| \vec{k},\ v\rangle\right|^2 \times (f_c - f_v)\,\pi\delta(E_c(\vec{k}+\vec{q}) - E_v(\vec{k}) - \hbar\omega); \tag{4}$$

f_v and f_c are Fermi distribution functions for valence and conduction bands:

$$f_v = (1 + e^{-E_F/k_BT})^{-1}, \quad f_c = (1 + e^{(\hbar\omega - E_F)/k_BT})^{-1};$$

E_c and E_v are conduction and valence band energies in Kane's[11] notation, that is

$$E_c(\vec{k}) = \tfrac{1}{2}(\eta + E_G), \tag{5}$$

$$E_v(\vec{k}) = 0, \tag{6}$$

$$\eta^2 = E_G^2 + \frac{8}{3}\frac{\hbar^2 k^2}{2m_0}E_p. \tag{7}$$

These relations hold for all x and T with[12]

$$E_G = -300 + 0.5T + (1910 - T)x \text{ meV}, \quad E_p = 18\,300 + 2700x \text{ meV}. \tag{8}$$

The matrix element in (4) can be calculated using wave functions given by Zawadzki and Szymanska[13]:

$$\left|\langle \vec{k}+\vec{q},\ c \left| e^{-i\vec{q}\cdot\vec{r}} \right| \vec{k},\ v\rangle\right|^2 = \frac{3}{8}\frac{\eta - E_G}{\eta}\frac{q^2\sin^2\theta}{|\vec{k}+\vec{q}|^2}, \tag{9}$$

θ is the angle between $\vec{k}$ and $\vec{q}$.

The matrix element (9) describes $\Gamma_8 \to \Gamma_8$ transitions in the semimetallic case ($E_G \leq 0$) and $\Gamma_8 \to \Gamma_6$ transitions in the semiconductor case ($E_G > 0$). Integration of these equations gives

$$\Delta\epsilon''_{\text{inter}}(\omega) = 2\left(\Re\frac{3}{2E_p}\right)^{1/2}\left(\frac{\hbar\omega - E_G}{\hbar\omega}\right)^{1/2}(f_v - f_c), \tag{10}$$

with

$$\Re = m_0e^4/2\hbar^2 = 13.6 \text{ eV}.$$

Equation (10) generalizes the parabolic-band model in both semimetallic and seimiconductor cases. $\Delta\epsilon''_{\text{inter}}(\omega)$ was calculated for a temperature of 8 K, at which our data were measured, and for degenerate samples.

The results of the calculations for $\Delta\epsilon''_{\text{inter}}(\omega)$ are shown in Fig. 1. In this figure, $N = 6\times10^{15}$ cm^{-3} except for pure CdTe where $N = 6\times10^{17}$ cm^{-3} in order to have $E_F - E_G > 4k_BT$. The real part of the interband contribution $\Delta\epsilon'_{\text{inter}}(\omega)$ is obtained by Kramers-Kronig inversion. Kane's model holds up to an energy E_1 of the order of $E_G + \frac{2}{3}\Delta$. Δ being the $\Gamma_8 - \Gamma_7$ splitting, that is about 1 eV above E_G.

To ensure convergence, the function to be integrated has been multiplied by a function of the form[14] $(E_s - \hbar\omega)/(E_s - E_1)$ with $E_s = 3E_1$ so that the result is independent of E_s within the required accuracy.

Figure 2 shows the result of the Kramers-Kronig inversion procedure on the curves of Fig. 1. Spectral regions corresponding to the energies of phonons are shown by a thick line for clarity. In this region $n^2 - k^2$ and $2nk$ usually vary in opposite direction with frequency, and this deepens the reflectivity minimum. Here, on the contrary, the slopes of $\Delta\epsilon'_{\text{inter}}$ and $\Delta\epsilon''_{\text{inter}}$ with frequency have the same sign. This qualitatively leads to an increase of reflectivity in the region of the minimum, as was noted before.[1]

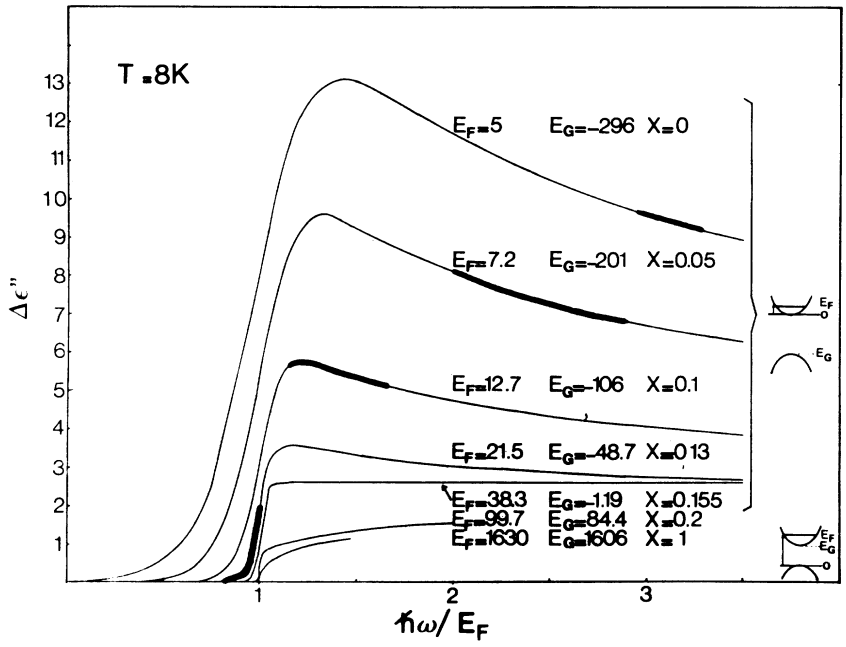

FIG. 1. Imaginary part of the contribution of $\Gamma_8 \rightarrow \Gamma_8$ transitions (semimetallic case) or $\Gamma_8 \rightarrow \Gamma_6$ transitions (semiconducting case) to the dielectric function of $Cd_xHg_{1-x}Te$ vs photon energy in reduced units $\hbar\omega/E_F$. Solid lines are computed from Eq. (10) as explained in text: E_F is the Fermi energy of electrons (meV) and E_G is the interaction energy gap (meV) as defined in Eq. (8). Negative E_G's refer to semimetallic band structure, positive values to semiconducting band structure. X is the molar fraction of CdTe in the crystal. Heavy lines give, for comparison, the location of phonon bands for each concentration.

The calculation of $\Delta\epsilon_{inter}$ within the framework of RPA only takes into account transitions between states with wave vector $\vec{k}$ and $\vec{k}+\vec{q}$ with $|\vec{q}|$ and $|\vec{k}| \ll 2\pi/a$. According to Alder,[15] local-field effects are not taken into account in this calculation. Those effects come from large-wave-vector components of the potential $e^{i(\vec{q}+\vec{G})\cdot\vec{r}}$, where $\vec{G}$ is a reciprocal-lattice vector. We further assume that those effects are constant and included in ϵ_∞. The polarization from valence to conduction bands transitions will not contribute to the local field acting on an ion but only to the macroscopic electric field.

B. Other contributions

Infrared[3-5,7,8] and Raman[6] data show that the $Cd_xHg_{1-x}Te$ series exhibits a "two-mode" behavior for the phonons of the mixed crystals. Several studies on those mixed crystals have been published.[16-18] All of them fail to account for this

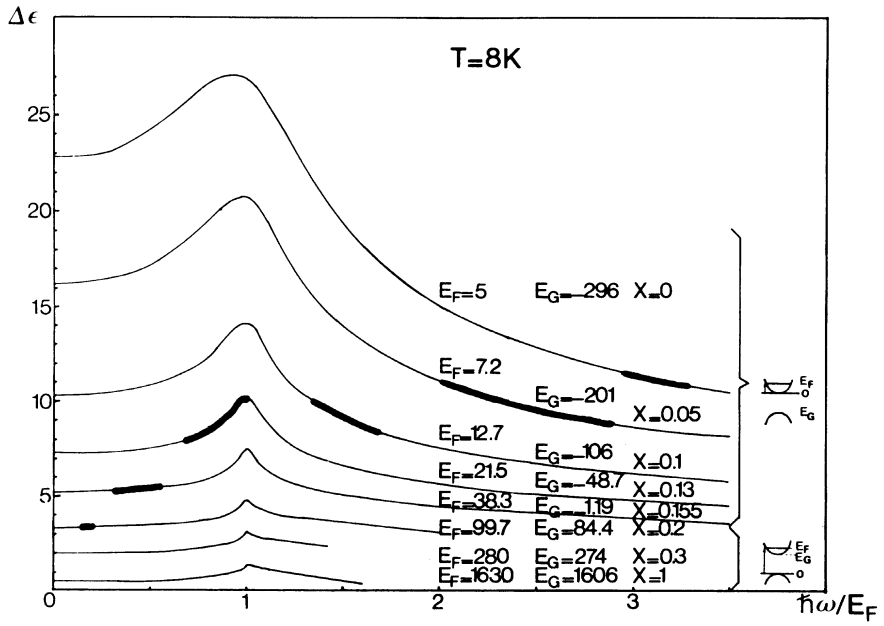

FIG. 2. Real part of $\Delta\epsilon_{inter}$ Vs $\hbar\omega/E_F$, obtained by a Kramers-Kronig inversion of $\Delta\epsilon''_{inter}$, as explained in text. Conditions and symbols same as in Fig. 1.

behavior or do so in a very incomplete fashion. This is due for a large part to the values used for the high-frequency dielectric constant in HgTe.

In this section, we present a model that accounts for the observed phonon spectrum and enables us to calculate the characteristic parameters of these phonons, including the contribution of plasmons and interband transitions.

In this model two types of sites are randomly distributed in the crystal: CdTe sites and HgTe sites with Nx of the first and $N(1-x)$ of the second per unit volume. In the equations of motion of ions, restoring forces F_i and effective charges e_i are linear functions of x. For the two types of sites, we can write

$$F_0(x) = F_0(0)\,(1+\theta_0 x)\,, \qquad F_1(x) = F_1(0)\,(1+\theta_1 x)\,, \tag{11}$$

and

$$e_0(x) = e_0(0)\,(1+\theta_0 x)\,, \qquad e_1(x) = e_1(0)\,(1+\theta_1 x)\,; \tag{12}$$

0 and 1 subscripts refer, respectively, to HgTe and CdTe.

The equations of motion for ions and free electrons will then be

$$\begin{aligned} \mu_0\ddot{u}_0 &= -F_0(x)u_0 - \mu_0\Gamma_0\dot{u}_0 + e_0(x)E_{\rm loc}\,,\\ \mu_1\ddot{u}_1 &= -F_1(x)u_1 - \mu_1\Gamma_1\dot{u}_1 + e_1(x)E_{\rm loc}\,,\\ m^*(E_F)\ddot{r} &= -m^*(E_F)\Gamma_e\dot{r} - eE\,. \end{aligned} \tag{13}$$

$m^*(E_F)$ is the effective mass of electrons at the Fermi level; μ_0 and μ_1 are the reduced masses of HgTe and CdTe; r is displacement of electrons; u_0 and u_1 are the relative displacement in each type of site; Γ_0, Γ_1, Γ_e are damping constants for ions and electrons; and E and $E_{\rm loc}$ are macroscopic and local electric fields.

Varga[19] showed that the polarization which comes into the relation between local and macroscopic fields does not contain the free-carrier contribution. The reason is that the wave vector of electrons is at most $\frac{1}{100}$ of the Brillouin zone, which means that the shortest response length for electrons is about 100 lattice parameters, whereas the ionic field varies rapidly over one unit cell. In the same way, interband transitions will not contribute to the local field and $E_{\rm loc}$ and E will be related by

$$E_{\rm loc} = E + \tfrac{4}{3}\pi P_R\,. \tag{14}$$

The lattice contribution P_R can be written

$$P_R = (1-x)\,N(x)\,e_0(x)\,u_0 + xN(x)\,e_1(x)\,u_1 + [(1-x)\,N(x)\,\alpha(0) + xN(x)\,\alpha(1)]\,E_{\rm loc}\,; \tag{15}$$

$N(x) = 4/a^3(x)$ is the number of ions per unit volume, $a(x)$ is the lattice constant, and $\alpha(0)$ and $\alpha(1)$ are the polarizability of elementary cells of each type.

Through the Lorentz-Lorenz transformation, one obtains from Eq. (15)

$$P_R = (1-x)\,N(x)\,e_0(x)\,u_0 + xN(x)\,e_1(x)\,u_1 + \left((1-x)\frac{N(x)}{N(0)}\frac{\epsilon_\infty(0)-1}{\epsilon_\infty(0)+2} + x\frac{N(x)}{N(1)}\frac{\epsilon_\infty(1)-1}{\epsilon_\infty(1)+2}\right)\frac{3}{4\pi}E_{\rm loc}\,. \tag{16}$$

A high-frequency dielectric constant $\epsilon_\infty(x)$ can then be defined

$$(1-x)\frac{N(x)}{N(0)}\frac{\epsilon_\infty(0)-1}{\epsilon_\infty(0)+2} + x\frac{N(x)}{N(1)}\frac{\epsilon_\infty(1)-1}{\epsilon_\infty(1)+2} = \frac{\epsilon_\infty(x)-1}{\epsilon_\infty(x)+2}\,. \tag{17}$$

With Eq. (17) and (14) one obtains

$$E_{\rm loc} = \frac{\epsilon_\infty(x)+2}{3}E + \frac{4\pi}{3}(1-x)\,N(x)\,e_0(x)\frac{\epsilon_\infty(x)+2}{3}u_0 + \frac{4\pi}{3}x\,N(x)\,e_1(x)\frac{\epsilon_\infty(x)+2}{3}u_1 \tag{18}$$

and

$$P_R = (1-x)\,N(x)\,e_0(x)\frac{\epsilon_\infty(x)+2}{3}u_0 + xN(x)e_1(x)\frac{\epsilon_\infty(x)+2}{3}u_1 + \frac{\epsilon_\infty(x)-1}{4\pi}e\,. \tag{19}$$

$E_{\rm loc}$ can then be replaced by its value in the equations of motion (13) in order to obtain expressions for u_0/E, u_1/E, and r/E.

The dielectric response to the macroscopic field is

$$D = \epsilon E = E + 4\pi P_T\,. \tag{20}$$

The total polarization P_T is

$$P_T = P_R - Ner + E\,\Delta\epsilon_{\rm inter}/4\pi\,. \tag{21}$$

Then

$$\epsilon(x,\omega) = \Delta\epsilon_{\rm inter}(x,\omega) + \epsilon_\infty(x) + 4\pi N(x)(1-x)\,e_0(x) \times \frac{\epsilon_\infty(x)+2}{3}\frac{u_0}{E} + 4\pi N(x)\,x\,e_1(x)\frac{\epsilon_\infty(x)+2}{3}\frac{u_1}{E} - 4\pi Ne\frac{r}{E}\,. \tag{22}$$

In order to solve the equations of motion we have to evaluate $\omega_0^2(x) = F_0(x)/\mu_0$; $\omega_1^2(x) = F_1(x)/\mu_1$; $e_0(x)$ and $e_1(x)$ for $x=0$ and $x=1$ [Eqs. (11) and (12)].

Szigeti effective charges are given by[20]:

$$\left(\frac{e_i}{e}\right)^2 = \frac{\epsilon_0(i)-\epsilon_\infty(i)}{4\pi N(i)}\,(\omega_{\rm TO}^2)_i\,4\pi^2c^2\mu_i\left(\frac{3}{\epsilon_\infty(i)+2}\right)^2 e^{-2}\,, \tag{23}$$

where μ_i is the reduced mass, $e = 4.8\times10^{-10}$ eV is the electron charge, c is the light velocity, and $\omega_{\rm TO}$ is the wave number of the transverse optical mode in $\rm cm^{-1}$. The value of $\omega_i^2(i)$ is given by

$$\omega_i^2(i) = (\omega_{\rm TO}^2)_i + \frac{4\pi N(i)}{3\mu_i}e_i^2(i)\frac{\epsilon_\infty(i)+2}{3}\,. \tag{24}$$

TABLE I. Numerical values for Eq. (24).

	$\epsilon_0-\epsilon_\infty$	$\omega_{TO}(cm^{-1})$	$a(10^{-8}$ cm)	$M(10^{-24}$ g)	ϵ_∞
HgTe	4.2	118.5	6.4616	129.5	12
CdTe	3.5	140	6.4810	99.27	8.5

Numerical values are given in Table I.

In this table, ϵ_∞ is a parameter, and the values which are given are selected for the best fit between theory and experiment. We then have: $e_0(0) = 0.54e$ and $e_1(1) = 0.68e$. With those values, we find

$$\omega_0^2(0) = 18\,253.97\ \text{cm}^{-2} = (135.1)^2\ \text{cm}^{-2},$$

$$\omega_1^2(1) = 26\,133.23\ \text{cm}^{-2} = (161.5)^2\ \text{cm}^{-2}.$$

To calculate θ, we need one more value which we estimated from Raman data[6] and infrared reflectivity.[5] We took $\omega_0(1) = 135\ \text{cm}^{-1}$ and $\omega_1(0) = 156.5\ \text{cm}^{-1}$, and obtained

$$\theta_0 = -0.002, \quad \theta_1 = 0.067.$$

The values for Γ_0 and Γ_1 are adjusted on the pure-compound values and Γ_e is calculated from mobility measurements:

$$\Gamma_0 = 4.5\ \text{cm}^{-1}, \quad \Gamma_1 = 5.8\ \text{cm}^{-1}, \quad \Gamma_e = 2\ \text{cm}^{-1}.$$

The dielectric function being completely determined, reflectivity curves can now be calculated and compared with experiment.

III. EXPERIMENTAL RESULTS

Our samples are $Cd_{0.13}Hg_{0.87}Te$. A 13% concentration of CdTe is one for which the interband $\Gamma_8 \rightarrow \Gamma_8$ contribution to $\epsilon(\omega)$ is still large since $E_G \simeq 50$ meV and the reststrahlen band of CdTe is still observable. At liquid-helium temperature, the free carrier concentration from low-field Hall effect is $(2 \pm 0.4) \times 10^{15}\ \text{cm}^{-3}$. Reflectivity versus wave number at 8 K is shown on Fig. 3. Reststrahlen bands corresponding to modified HgTe and CdTe modes exhibit relative intensities roughly proportional to the concentration of each constituent.

In Fig. 4 the two parts of the dielectric function are plotted for 8 K since at this temperature plasmon modes are too low in energy ($\omega \simeq 40\ \text{cm}^{-1}$) to allow Kramers-Kronig analysis from our results, which do not cover this range. Maxima of $\epsilon'' = 2nk$ correspond to dissipative (transverse) modes. The larger peak comes from HgTe modes with $\omega_1 = 119.5\ \text{cm}^{-1}$, and the smaller from CdTe at $\omega_2 = 153.5\ \text{cm}^{-1}$; those frequencies being, of course, different from those of pure constituent compounds.

Maxima of $\text{Im}(-\epsilon^{-1})$ give the frequencies of longitudinal modes at 131.5 cm^{-1} (HgTe) and 155 cm^{-1} (CdTe). In these two curves, the interband contribution $\Delta\epsilon_{\text{inter}}$ was taken into account (Fig. 5)

IV. DISCUSSION

The experimental results near the semimetal-semiconductor transition concentration and the analysis of the interband contribution allow us to explain the infrared spectrum of $Cd_xHg_{1-x}Te$ for any x and particularly near the band crossing point. Our working hypothesis was that the adiabatic approximation is sufficient to account for the behavior of lattice modes in this series for all x. Confrontation of our simple model with experiment entirely confirms this assumption.

Examination of Figs. 3 and 6 clearly shows the importance of the frequency dependence of the interband contribution. It has been previously shown in[1] HgTe that omitting this variation led to

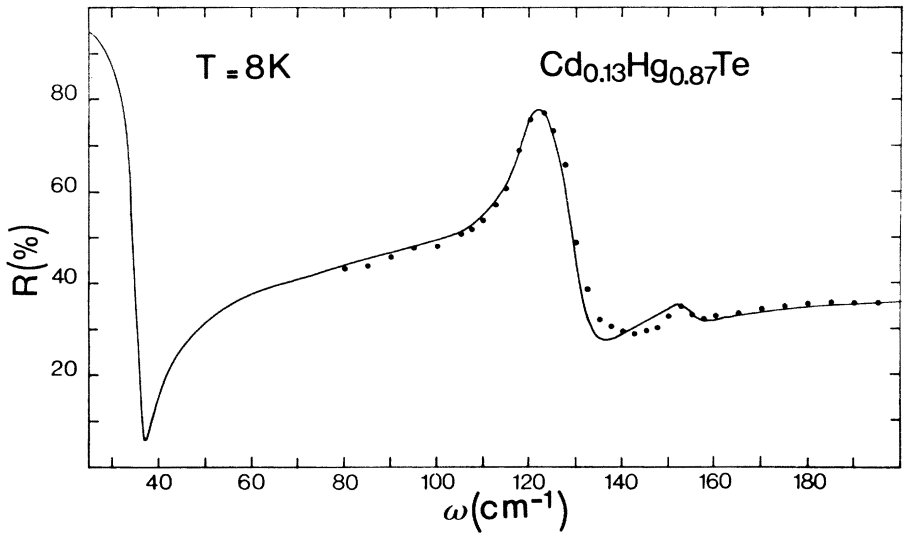

FIG. 3. Experimental reflectivity (dots) versus wave number for $x = 0.13$ compared with theory (solid line). The parameters used for the calculation are those of Table I and $\Delta\epsilon_{\text{inter}}(\omega)$ is taken into account.

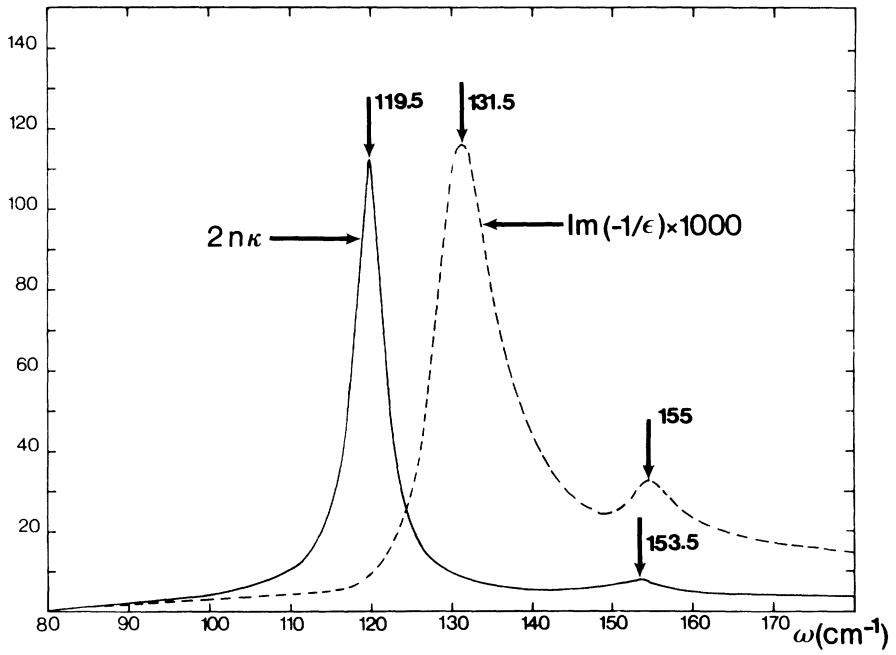

FIG. 4. Im(ϵ) (dashed line) corresponding to transverse modes and Im $(-\epsilon^{-1})$(solid line) to longitudinal modes versus wave number for $x = 0.13$ at 8 K.

impossibilities in analyzing experimental results. In the present case where the variation of $\Delta\epsilon'_{inter}$ and $\Delta\epsilon''_{inter}$ is large in the reststrahlen regions, using a real constant value for $\epsilon_\infty + \Delta_{inter}$ will not permit a fit of the reflectivity curve in this experiment. This is especially obvious in the region of the reflectivity minimum, the fit of which would be completely outside experimental uncertainty without introduction on the actual interband contribution.

Regarding the model used here for lattice vibrations in mixed crystals, one should note that long-wavelength optical modes in $AB_{1-x}C_x$ mixtures have been analyzed along several phenomenological approaches. The random-element-isodisplacement model is most currently used. Here it is modified to take into account long-distance interactions. In this mode, cations and anions of the same kind oscillate with the same phase and amplitude. In a quasi unit cell containing one A ion, $1-x$ B ions, and x C ions, force constants between first neighbors $F_{AB}(x)$ and $F_{AC}(x)$ vary with con-

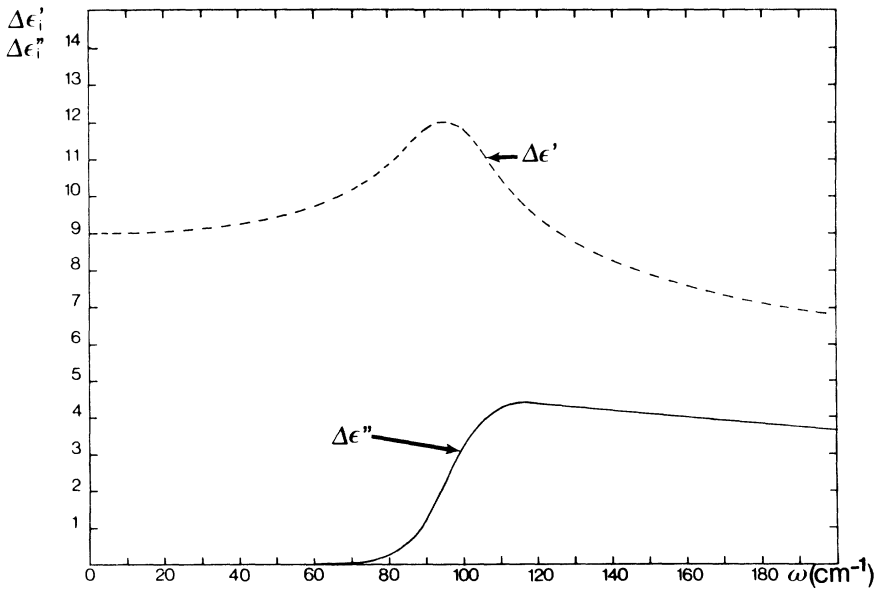

FIG. 5. Real and imaginary parts of the contribution of $\Gamma_8 \rightarrow \Gamma_8$ transitions to the dielectric function versus wave number for $x = 0.13$ and $T = 8$ K: $\Delta\epsilon'_{inter}$ dashed line, $\Delta\epsilon''_{inter}$ solid line.

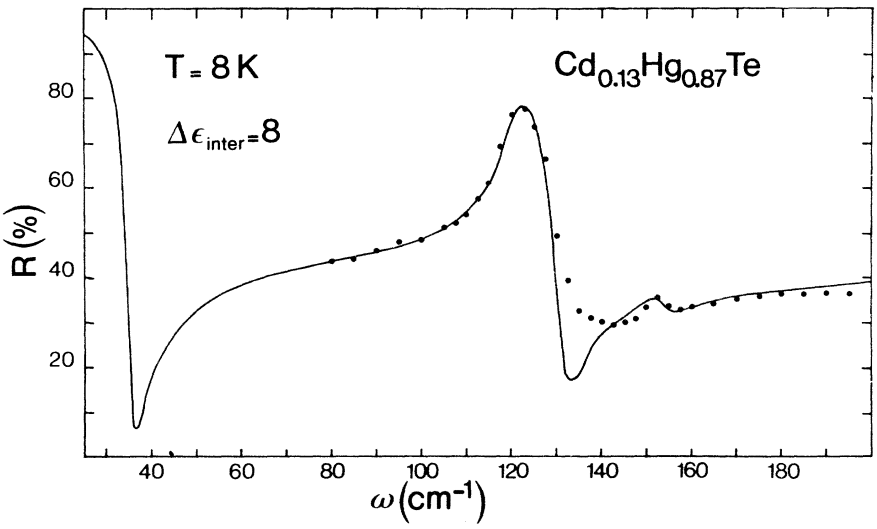

FIG. 6. Experimental reflectivity (dots) compared with a theory when using real and constant value for $\Delta\epsilon_{inter}$. All other parameters are identical to those of Fig. 3. This curve is intended to show that it is not possible to fit the experimental behavior with theory without taking into account the real shape of the interband contribution (cf. Fig. 3).

centration and can be determined from transverse-mode frequencies ω_T in pure crystals. The second-neighbor force constant $F_{BC}(x)$ is adjusted on the values of impurity (local or gap) modes ω_1. All those force constants are computed from the two limiting cases ($x=0$ and $x=1$). With this model for $Cd_xHg_{1-x}Te$, one obtains

$$F_0(0)/\mu_0 = \omega_0^2(0) = (135.1)^2\ \text{cm}^{-2},$$

$$F_1(1)/\mu_1 = \omega_1^2(1) = (161.5)^2\ \text{cm}^{-2},$$

$$\frac{F_1(0)+F_{CdHg}(0)}{m_{Cd}} = \omega_I^2(\text{CdTe}) = (156.5)^2\ \text{cm}^{-2},$$

$$\frac{F_0(1)+F_{CdHg}(1)}{m_{Hg}} = \omega_I^2(\text{HgTe}) = (135)^2\ \text{cm}^{-2}.$$

Then

$$\frac{F_{CdHg}}{m_{Hg}} = \omega_I^2(\text{HgTe}) - \omega_0^2(0) + \frac{F_0}{m_{Te}} \simeq \frac{F_0}{m_{Te}},$$

$$\frac{F_{CdHg}}{m_{Cd}} = \omega_I^2(\text{CdTe}) - \omega_1^2(1) + \frac{F_1}{m_{Te}} \simeq \frac{F_1}{m_{Te}}.$$

Thus one would get for second-neighbor forces

$$F_{CdHg} \simeq 1.6F_0 \simeq 0.9F_1.$$

In this model, second-neighbor forces between ions of the same sign of the same order of magnitude or longer than forces between first neighbors with opposite signs. For this reason we did not use it, being unrealistic.

V. CONCLUSION

In this work, we studied the optical properties of $Cd_xHg_{1-x}Te$ mixed crystals in the vicinity of the semimetal-semiconductor transition ($x \simeq 0.13$) at 8 K in the far infrared (40 – 125 μm). Our results show that using the adiabatic approximation still allows a correct description of lattice modes in those compounds.

The interband contribution to the dielectric function which corresponds to transitions from the heavy-hole band to the conduction band ($\Gamma_8 \rightarrow \Gamma_8$ on the HgTe side; $\Gamma_8 \rightarrow \Gamma_6$ on the CdTe side) has been computed in the frame of Kane's procedure, taking into account nonparabolicity.

Our model for the phonon contribution for all x accounts for the two-mode behavior of those compounds, in contrast with previous calculations. All our conclusions apply both to the semimetallic and to the semiconductor case.

ACKNOWLEDGMENTS

It is a pleasure to acknowledge Dr. W. Giriat from the University of Warsaw, which provided us with the samples, and Dr. M. Grynberg (University of Warsaw) for stimulating discussions.

[1]M. Grynberg, R. Letoullec, and M. Balkanski, Phys. Rev. B 9, 517 (1974).

[2]J. G. Broerman, in *Proceedings of the Eleventh International Conference on the Physics of Semiconductors* (PWN-Polish Scientific Publishers, Warsaw, 1972), p. 917.

[3]R. S. Kim and S. I. Narita, J. Phys. Soc. Jpn. 31, 613 (1971).

[4]J. R. Birch, Infrared Phys. 12, 29 (1972).

[5]J. Baars and F. Sorger, Solid State Commun. 10, 875 (1972).

[6]A. Mooradian and T. C. Harman, *The Physics of Semi-Metals and Narrow Gap Semiconductors*, Dallas 1970, edited by D. L. Carter and R. T. Bate (Pergamon, New York, 1971), p. 297.

[7]D. L. Carter, M. A. Kinch, and D. D. Buss, in Ref. 6, p. 273.

[8]M. A. Kinch and D. D. Buss, in Ref. 6, p. 461.

[9]J. Blinowski, Rapport Scientifique du Laboratoire de Physique des Solides No. 10, 1974. (unpublished).
[10]In our calculation of the interband contribution it was not necessary to derive the exact shape of the light-holes conduction-band contribution since those transitions occur at an energy $E_G + 2E_F$ of 80 meV for our samples. This energy is outside the range that we studied here (20 meV). Absorption due to those transitions is weak in this domain and their contribution is taken care of in the constant high-energy part of the dielectric function.
[11]E. O. Kane, J. Phys. Chem. Sol. 1, 249 (1957).
[12]J. D. Wiley and R. N. Dexter, Phys. Rev. 181, 1181 (1961).
[13]W. Zawadski and W. Szymańska, Phys. Status Solidi B 45, 415 (1971).
[14]E. Stern, Phys. Rev. 133, A1653 (1964).
[15]S. L. Adler, Phys. Rev. 126, 413 (1962).
[16]R. Beserman, Ann. Phys. (Paris) 4, 197 (1969).
[17]I. F. Chang and S. S. Mitra, Adv. Phys. 20, 359 (1971).
[18]H. Harada and S. I. Narita, J. Phys. Soc. Jpn. 30, 1628 (1971).
[19]B. B. Varga, Phys. Rev. 137, A1896 (1965).
[20]R. Letoullec, thèse (University of Paris, 1968) (unpublished).